

Damage-Associated Molecular Patterns Induce Inflammatory Injury During Machine Preservation of the Liver: Potential Targets to Enhance a Promising Technology

Uwe Scheuermann,¹ Minghua Zhu,¹ Mingqing Song,¹ John Yerxa,¹ Qimeng Gao,¹ Robert P. Davis,¹ Min Zhang,¹ William Parker,¹ Matthew G. Hartwig,¹ Jean Kwun,¹ Todd V. Brennan,² Jaewoo Lee,¹ and Andrew S. Barbas^{1*}

¹Department of Surgery, Duke University Medical Center, Durham, NC; and ²Department of Surgery, Cedars-Sinai Medical Center, Los Angeles, CA

Machine preservation (MP) has emerged as a promising technology in liver transplantation, but the cellular processes occurring during MP have not been characterized. Recent studies have noted the presence of inflammatory molecules generated during MP. We hypothesized that there is a metabolism-dependent accumulation of damage-associated molecular patterns (DAMPs) and inflammatory cytokines during MP and that these molecules provoke inflammation in the graft. To stratify groups by metabolic rate, MP was performed on rat livers from standard donors at 3 different temperatures: room temperature (RT), subnormothermic (30°C), and normothermic (37°C). Static cold storage at 4°C was included as a reference group. Following a 4-hour preservation period, graft reperfusion was performed *ex vivo* at 37°C (n = 6 for all groups). Levels of DAMPs and inflammatory cytokines were measured, and their biological activity was assessed by determining toll-like receptor (TLR) stimulation, inflammatory gene expression, and activation of cell death pathways. There was a time-dependent increase in levels of DAMPs during MP with high-mobility group box 1 and extracellular DNA levels increasing for all groups ($P < 0.05$, 30 versus 240 minutes). Tumor necrosis factor α levels in the perfusate also increased during MP for all groups ($P < 0.05$, 30 minutes versus 240 minutes). Levels of inflammatory molecules correlated with increased activation of TLRs (TLR3, $P = 0.02$, normothermic machine preservation [MP37] versus machine preservation at room temperature [MPRT]; TLR9, $P = 0.02$, MP37 versus MPRT). Priming of the NLRP3 inflammasome and activation of cell death pathways were reduced in grafts preserved by MP at room temperature. In conclusion, inflammatory molecules produced during MP have a biological impact on the graft. Therapies to attenuate DAMP-mediated inflammation during MP may further enhance this promising technology.

Liver Transplantation 25 610–626 2019 AASLD.

Received October 2, 2018; accepted January 24, 2019.

Machine preservation (MP) has emerged as a promising organ preservation strategy in liver transplantation, particularly for extended criteria donors. Several

preclinical and clinical studies have established the safety and efficacy of MP in both hypothermic and normothermic systems.⁽¹⁻⁵⁾ Recently, a European randomized clinical trial demonstrated a reduction in posttransplant peak aspartate aminotransferase (AST) and early allograft dysfunction for livers preserved by normothermic MP in comparison to cold storage.⁽⁶⁾

Although the clinical use of MP has progressed rapidly, our understanding of the physiologic processes occurring in this environment remains limited. Although MP restores cellular metabolism by perfusing the graft with nutrients and oxygen, it does not fully recapitulate the complexity of a living organism.

Abbreviations: ALT, alanine aminotransferase; AST, aspartate aminotransferase; DAMP, damage-associated molecular pattern; ELISA, enzyme-linked immunosorbent assay; exDNA, extracellular DNA; GAPDH, glyceraldehyde 3-phosphate dehydrogenase; H & E, hematoxylin-eosin; HEK, human embryonic kidney; HMGB1, high-mobility group box 1; HO-1, heme oxygenase 1; IL, interleukin; I-R, ischemia/reperfusion; LDH, lactate dehydrogenase; MLKL, mixed lineage kinase domain-like protein; MP, machine preservation;

One notable limitation of current systems in clinical use is the absence of renal filtration. MP devices continuously recirculate perfusate, with no mechanisms to maintain electrolyte homeostasis, eliminate metabolic products, or clear inflammatory molecules.

Recent studies have demonstrated the accumulation of inflammatory cytokines during MP, attributed to release by tissue resident leukocytes.^(7,8) Moreover, graft cells injured during the ischemia/reperfusion (I-R) process release various damage-associated molecular patterns (DAMPs) into the perfusate.⁽⁹⁾ DAMPs are a heterogeneous collection of molecules released by injured and dying cells that bind to distinct pattern-recognition receptors on tissue resident leukocytes and graft cells, initiating proinflammatory responses.^(10,11)

The biological significance of these inflammatory molecules during MP is unknown. We hypothesized that there is a metabolism-dependent accumulation of DAMPs and cytokines during MP and that

these molecules mediate inflammation in the graft. Thus, the objectives of this study were to investigate DAMP and cytokine release during MP and to determine downstream effects on toll-like receptor (TLR) signaling, NLR family pyrin domain containing 3 (NLRP3) inflammasome activation, and cell death after reperfusion.

Materials and Methods

ANIMALS

Male Sprague Dawley rats (Charles River Laboratories, Wilmington, MA), weighing 296 ± 8 g (mean \pm standard error of the mean [SEM]), were used for the experiments. All animals were housed in specific pathogen-free conditions in the animal care facilities at the Duke University Medical Center in accordance with institutional guidelines. All animals received humane care and procedures were approved by the Institutional Animal Care and Use Committee at Duke University.

STUDY DESIGN

The primary objective of this study was to characterize inflammation during MP and define how this affects graft function following reperfusion. To probe the effects of metabolic rate, different temperatures were used during MP. Rats were randomly separated into groups ($n = 6$) by MP temperature: machine preservation at room temperature (MPRT; $25^{\circ}\text{C} \pm 0.1$), subnormothermic machine preservation (MP30; 30°C), or normothermic machine preservation (MP37; 37°C). A reference group of static cold storage (SCS; 4°C) was also tested. All livers were preserved for 4 hours, followed by ex vivo reperfusion, as described subsequently (Fig. 1).

EXPERIMENTAL PROCEDURES

Liver Procurement

All surgeries were performed under cone mask anesthesia with continuous 5% isoflurane (Isothesia, Henry Schein Animal Health, Melville, NY) for induction, and 2%–3% isoflurane during the procedure with 2 L/minute oxygen flow. The abdominal cavity was opened by a midline and transverse incision. A stent fashioned from a 24-gauge angiocatheter (BD Insyte autoguard Becton Dickinson, Franklin Lakes, NJ) was inserted into the common bile duct and secured. The proper

MP30, subnormothermic machine preservation; MP37, normothermic machine preservation; MPRT, machine preservation at room temperature; MyD88, myeloid differentiation protein 88; Nfe2l2, nuclear factor (erythroid-derived 2)-like 2; NF- κ B, nuclear factor kappa B; NLRP3, NLR family pyrin domain containing 3; OER, oxygen extraction ratio; PARP, poly(adenosine diphosphate ribose) polymerase; pMLKL, phosphorylated mixed lineage kinase domain-like protein; RT, room temperature; SCS, static cold storage; SDHA, succinate dehydrogenase complex flavoprotein subunit A; SEAP, secreted embryonic alkaline phosphatase; SEM, standard error of the mean; SOD, superoxide dismutase; TLR, toll-like receptor; TNF- α , tumor necrosis factor α ; TUNEL, terminal deoxynucleotidyl transferase-mediated deoxyuridine triphosphate nick-end labeling; UW, University of Wisconsin.

Address reprint requests to Andrew S. Barbas, M.D., Department of Surgery, Duke University Medical Center, DUMC Box 3512, Durham, NC 27710. Telephone: 919-668-2424; FAX: 919-684-8716; E-mail: andrew.barbas@duke.edu

This work was supported by the American Society of Transplant Surgeons–Astellas Faculty Development Grant.

© 2019 The Authors. Liver Transplantation published by Wiley Periodicals, Inc., on behalf of American Association for the Study of Liver Diseases. This is an open access article under the terms of the Creative Commons Attribution-NonCommercial License, which permits use, distribution, and reproduction in any medium, provided the original work is properly cited and is not used for commercial purposes.

View this article online at wileyonlinelibrary.com.

DOI 10.1002/lt.25429

Potential conflict of interest: Nothing to report.

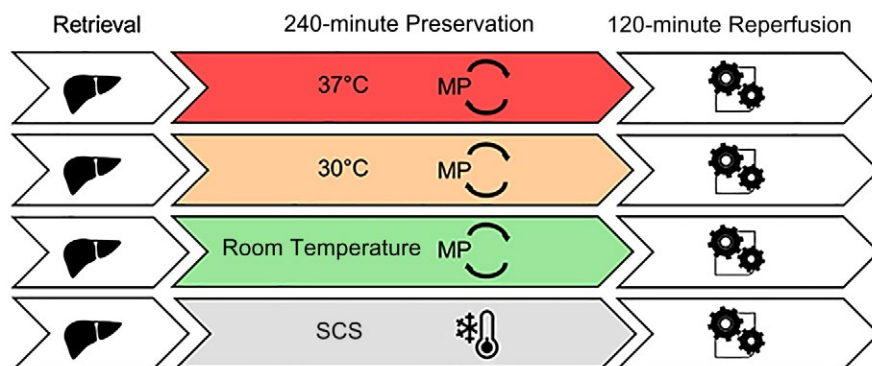


FIG. 1. Experimental design. Standard criteria rat livers were preserved for 4 hours by either SCS (4°C) or MPRT (25°C), MP30 (30°C), or MP37 (37°C). Following 4 hours of preservation, livers were then reperfused ex vivo at 37°C for 2 hours using Krebs-Henseleit buffer.

hepatic artery and gastrosplenic and duodenopancreatic branches of the portal vein were isolated and divided. Heparin (1 IU/g bodyweight, Fresenius Kabi, Lake Zurich, IL) was injected through the infrahepatic vena cava with a 30-gauge needle. Then, 5 minutes later, the portal vein was cannulated with a perfusion cannula (Harvard Apparatus, Holliston, MA), and the liver was gently flushed with 40 mL of cold University of Wisconsin (UW) solution (Bridge of Life, Columbia, SC). The liver was then explanted and weighed.

Static Cold Storage

For SCS, grafts were immersed in UW solution (Bridge of Life) at 4°C for 4 hours.

Ex Vivo MP

Ex vivo MP was performed in a recirculating system consisting of a perfusate reservoir, an autoclavable organ chamber (Type 834/10), an oxygenator, a peristaltic pump, and a bubble trap (Hugo Sachs Elektronik, March-Hugstetten, Germany). The chamber was enclosed in a conditioning system that allows precise regulation and control of the temperature (Optima T100, Grant instruments, Beaver Falls, PA). A leukocyte filter (EZ Prime, Haemonetics, Braintree, MA) was used to capture circulating inflammatory cells in the perfusate. The total perfusate volume was 100 mL, consisting of 80 mL of Williams' Medium E (Sigma-Aldrich, St. Louis, MO), supplemented with 5% bovine serum albumin (Hyclone, GE Healthcare Life Sciences,

South Logan, UT), and 20 mL of type O+ human red blood cells (American Red Cross, Durham, NC). Additives included 0.2 U of insulin (Humulin; Eli Lilly, Indianapolis, IN), 29.2 mg of L-glutamine (L-Glutamine [200 nM]; Life Technologies, Grand Island, NY), 1 mg of hydrocortisone (Solu-Cortef; Pfizer, New York, NY), and 500 IU of heparin (Fresenius Kabi). The perfusate used in these experiments was based on previously published perfusates for normothermic ex vivo MP.^(12,13) The peristaltic pump (Harvard Apparatus) generated a continuous perfusate flow and liver perfusion through the portal vein with a flow rate of 1.80 mL/minute/g liver. The oxygenator was gassed with a mixture of 95% O₂ and 5% CO₂ (Airgas, Durham, NC).

Graft Reperfusion

After preservation by either MP or SCS, grafts were transferred directly to the perfusion circuit and subsequently reperfused ex vivo for 2 hours. Grafts were not flushed prior to reperfusion to minimize graft manipulation. The reperfusion circuit setup was mechanically identical to the preservation circuit. Reperfusion media consisted of 100 mL of oxygenated (95% O₂ and 5% CO₂) Krebs-Henseleit buffer (Sigma-Aldrich) supplemented with 5% bovine serum albumin. Mean (\pm SEM) perfusate flow rate was 2.84 ± 0.04 mL/minute/g liver, and temperature was maintained at 37°C. Before reperfusion, the liver was allowed to equilibrate for 15 minutes to simulate the performance of vascular anastomoses (equilibration phase).

ANALYTICAL METHODS

Intrahepatic Vascular Resistance

The intrahepatic vascular resistance was calculated as portal vein pressure (mm Hg)/perfusate flow rate (mL/minute). During MP and reperfusion, portal vein pressure was measured continuously (Flow pressure transducer P75, HSE amplifier module TAM-D; Hugo Sachs Elektronik). LabChart Pro software (AD Instruments, Colorado Springs, CO) was used to display and record flow rates and portal vein pressure.

Blood Gas Analysis

Perfusate samples were drawn from the portal venous inflow and from the suprahepatic caval outflow at different time points for blood gas analysis using a point-of-care device (iSTAT, CG4+ cartridges, Abbott Point of Care Inc., Abbott Park, IL). Measurements included lactate concentration and acid-base parameters (pH, HCO_3^- , base excess, partial pressure of oxygen, and partial pressure of carbon dioxide).

Calculation of Oxygen Extraction Ratio and Oxygen Consumption Rate

The oxygen extraction ratio (OER) during MP was calculated using the following equation: $\text{OER} = [(S_i\text{O}_2 - S_o\text{O}_2)/S_i\text{O}_2] \times 100$, where $S_i\text{O}_2$ represents the oxygen saturation of the inflow (portal vein) and $S_o\text{O}_2$ represents the oxygen saturation of the outflow (suprahepatic vena cava).

The oxygen consumption rate during reperfusion was calculated using the following equation: oxygen consumption rate ($\mu\text{L}/\text{minute}/\text{g}$ liver) = perfusate flow $\times S \times (P_i\text{O}_2 - P_o\text{O}_2)/\text{g}$ liver (S , solubility constant of oxygen in water at $37^\circ\text{C} = 0.031 \mu\text{L}/\text{mL}/\text{mm Hg}$).

Bile Processing and Analysis

Bile was collected throughout MP, and volume was determined hourly. Bile was transferred to 1-mL Corning cryogenic vials (VWR, Atlanta, GA), frozen with liquid nitrogen, and stored at -80°C for subsequent analysis. Biliary lactate dehydrogenase (LDH) was determined using a rat LDH enzyme-linked immunosorbent assay (ELISA) kit (LifeSpan BioSciences, Seattle, WA), and biliary glucose was analyzed with the iSTAT point-of-care device (Chem8+ cartridges; Abbott Point of Care).

Perfusate Analysis

At different time points, 2 mL of perfusate was collected and centrifuged at 2500 rpm at 4°C for 15 minutes to remove cellular debris. The supernatant was transferred to 1-mL Corning cryogenic vials immediately after centrifugation, frozen with liquid nitrogen, and stored at -80°C for subsequent analysis.

Transaminase Release

AST and alanine aminotransferase (ALT) in perfusate were measured using a Piccolo Xpress Chemistry Analyzer (Abaxis, Union City, CA).

DAMP Levels

Levels of extracellular DNA (exDNA) were determined using Quant-iT PicoGreen double-stranded DNA kit (Molecular Probes, Eugene, OR). High-mobility group box 1 (HMGB1) levels were determined by ELISA (IBL, Hamburg, Germany).

TLR Activation

TLR activation was measured using TLR reporter cell lines human embryonic kidney (HEK)-hTLR3, HEK-hTLR4, and HEK-hTLR9 cells (InvivoGen, San Diego, CA), stably expressing a nuclear factor kappa B (NF- κ B)/activator protein 1-inducible secreted embryonic alkaline phosphatase (SEAP). All cells were grown in Dulbecco's modified Eagle's medium supplemented with 10% fetal bovine serum at 37°C in a humidified atmosphere with 5% CO_2 . Perfusates were diluted to 15% (vol/vol) in growth media and incubated with TLR reporter cells in flat-bottom 96-well plates for 16 hours. SEAP levels were then determined by colorimetric assay using QUANTIBLue assay (InvivoGen). Polyinosinic:polycytidylic acid (5 $\mu\text{g}/\text{mL}$, InvivoGen), lipopolysaccharide (20 ng/mL , Sigma-Aldrich), and CpG (1 mM, InvivoGen) were used as TLR3, TLR4, and TLR9 stimulator controls, respectively. Culture media from stimulated HEK-null cell lines (InvivoGen) were used as negative controls.

Cytokine Levels

Perfusate interleukin (IL) 1 α , IL2, IL4, and tumor necrosis factor α (TNF- α) levels were measured by flow cytometry using BD Cytometric Bead Array Rat Flex sets (BD Bioscience, San Jose, CA) on a BD LSRFortessa X-20 analyzer (BD Bioscience). IL6 levels were measured by ELISA (Sigma-Aldrich).

Liver Tissue Processing

Liver parenchyma was either immersed in RNAlater Solution (Thermo Fisher Scientific, Waltham, MA) and frozen at -80°C for later RNA isolation or fixed in 10% formalin for histologic assessment.

RNA Extraction and Quantitative Polymerase Chain Reaction

Total RNA from frozen liver samples was isolated using the QIAshredder and RNeasy Mini-Kit (Qiagen, Hilden, Germany). The resultant RNA was quantified using NanoDrop 2000 Spectrophotometer (Thermo Fisher Scientific). Subsequently, equal amounts of RNA were converted to complementary DNA with the iScript complementary DNA Synthesis Kit (Biorad, Hercules, CA). Taq-Man gene expression assays (Applied Biosystems, Foster City, CA) were performed using the following primers: NF- κ B (Rn01399572_m1), myeloid differentiation protein 88 (MyD88; Rn01640049_m1), TNF- α (Rn99999017_m1), NLRP3 (Rn04244620_m1), IL1 β (Rn00580432_m1), IL18 (Rn01422083_m1), IL6 (Rn01410330_m1), nuclear factor (erythroid-derived 2)-like 2 (Nfe2l2) (Rn00582415_m1), heme oxygenase 1 (HO-1; Rn00561387_m1), superoxide dismutase (SOD)-2 (Rn00690588_g1), and succinate dehydrogenase complex flavoprotein subunit A (SDHA; Rn00590475_m1). All samples were analyzed in triplicate. Amounts of specific messenger RNA were normalized to the individual quantities of transcripts of SDHA. The expression of SDHA remained constant in the experimental groups.

Western Blot Analysis

Rat livers either freshly isolated or following graft reperfusion were frozen in RNAlater (Thermo Fisher Scientific) at -80°C . Protein from liver pieces was then extracted using Cell Disruption Buffer from PARIS Kit (Life Technologies); 10–20 μg of total protein from each sample was separated on sodium dodecyl sulfate–polyacrylamide gel electrophoresis and transferred to a nitrocellulose membrane. Antibodies used for Western blotting included the following: anti-poly(adenosine diphosphate ribose) polymerase (PARP) antibody (#9542; Cell Signaling Technology, Danvers, MA), anti-phosphor S345 mixed lineage kinase domain-like protein (MLKL; ab196436; Abcam, Cambridge, MA), and anti-glyceraldehyde 3-phosphate dehydrogenase

(GAPDH; ab181602; Abcam). Bound antibodies on membranes were removed using Restore Plus Western Blot Stripping Buffer (Thermo Fisher Scientific) when additional Western blotting was needed.

Histology

Liver tissue was fixed in 10% formalin and embedded in paraffin. Sections were obtained from the medial left lateral lobe. Paraffin sections were stained with hematoxylin-eosin (H & E) for morphologic observation. Severity of histological damage was blindly scored by Suzuki criteria after H & E staining. Sinusoidal congestion, hepatocyte necrosis, and ballooning degeneration were graded from 0 to 4 points, and the final score is the sum of the grades for each item, as previously described.⁽¹⁴⁾ Immunohistochemical staining for cleaved caspase 3 (Cell Signaling Technology) and terminal deoxynucleotidyl transferase–mediated deoxyuridine triphosphate nick-end labeling (TUNEL; Roche Diagnostics GmbH, Mannheim, Germany) were used to demonstrate apoptosis.⁽¹⁵⁾ Whole slide digital images were captured by using the Aperio AT Turbo digital slide scanner system (Leica Biosystems, Vista, CA). Quantitative immunohistochemical analysis was performed using Aperio Imagescope (Leica Biosystems) digital pathology software. Apoptosis index was calculated by pixel positivity of cleaved caspase 3 and TUNEL labeling cells in the measured areas.

STATISTICAL ANALYSIS

Graphpad Prism software, version 7.04 (GraphPad Software Inc., La Jolla, CA) was used for statistical analyses and graphs. All values are presented as mean \pm SEM. Differences between continuous values were analyzed using unpaired Student *t* test. The Mann-Whitney U test was used for evaluation of the Suzuki score. *P* values <0.05 were considered significant.

Results

INDICES OF GRAFT FUNCTION DURING MP AND REPERFUSION

Oxygen Utilization Increases With Temperature During MP

The OER, defined as the ratio of oxygen consumption (VO_2) to oxygen delivery (DO_2), was measured

during MP. Normal values of OER are in the 20%-30% range, and an OER below normal indicates either decreased oxygen consumption or excessive delivery. Conversely, an OER above normal indicates either increased oxygen consumption or inadequate delivery.⁽¹⁶⁾

During 4 hours of MP, the mean OER was at or below the normal range in all groups, indicating that

oxygen delivery was adequate. A temperature-dependent effect on OER was observed, reflecting increased oxygen consumption with increased temperature, as expected (Fig. 2A).

During graft reperfusion, different trends in oxygen utilization were observed. By 30 minutes into graft reperfusion, mean oxygen consumption was

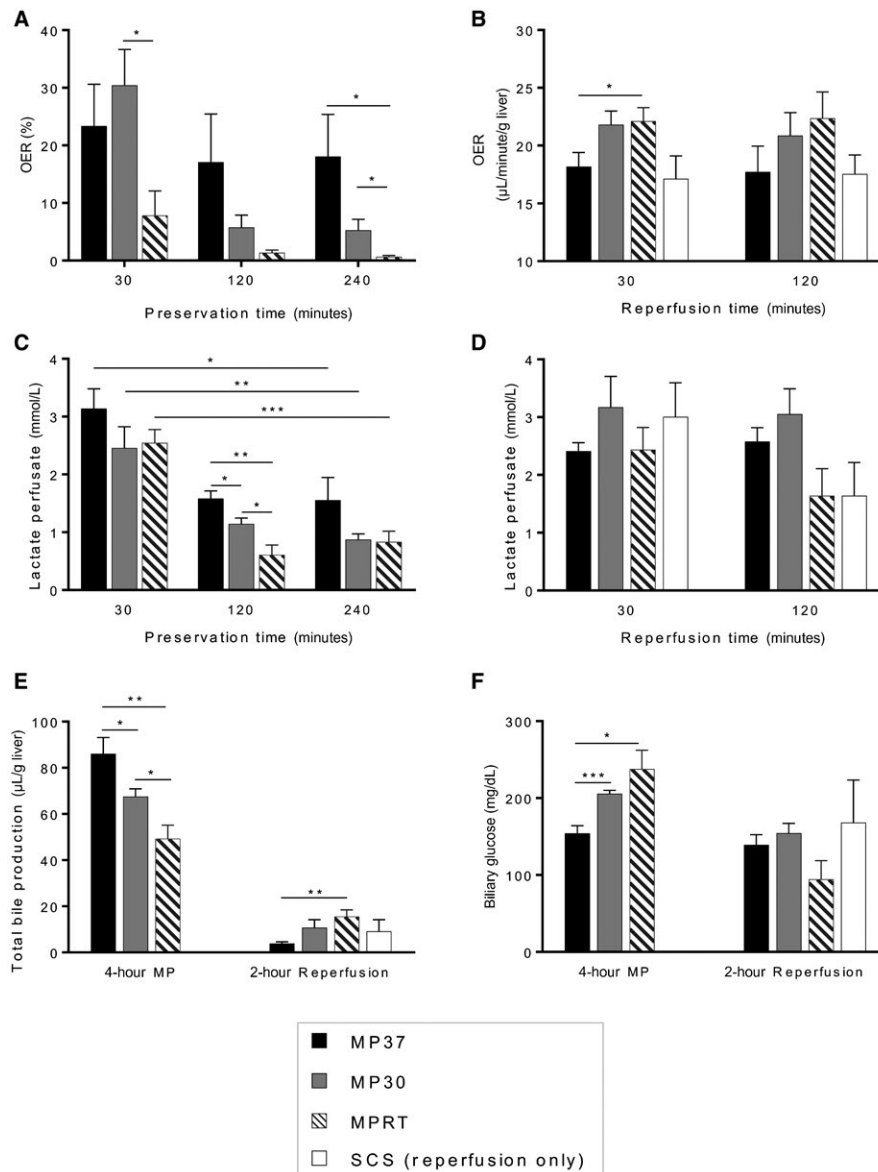


FIG. 2. Graft function during MP and reperfusion. (A) OER was greater at higher temperatures during MP, reflecting an increased graft metabolic rate. (B) During reperfusion, oxygen consumption was highest for livers preserved by MPRT. (C) Lactate levels in the perfusate decreased to low levels for all groups during MP. (D) During reperfusion, lactate levels trended lower for MPRT and SCS groups but did not reach significance. (E) Bile production during MP was proportional to temperature and metabolic rate. During reperfusion, bile production was greatest for livers that had been preserved by MPRT. (F) Biliary glucose levels during MP were lowest for MP37, indicating greater reabsorption by the biliary epithelium. During reperfusion, there was a trend toward lower biliary glucose in the MPRT group ($P = 0.06$, MPRT versus MP30). Data are shown as mean \pm SEM, $n = 6$ per group. * $P < 0.05$, ** $P < 0.01$, *** $P < 0.001$.

highest for the MPRT group, indicating greater metabolic activity of these grafts ($P = 0.04$, MPRT versus MP37; Fig. 2B). By 120 minutes of reperfusion, no significant difference in mean oxygen consumption between groups was observed, although a trend toward increased oxygen consumption continued to be present in the MPRT group ($P = 0.10$, MPRT versus SCS; Fig. 2B).

Grafts Metabolize Lactate During MP

Lactate levels in the perfusate were measured during MP, reflecting a balance between anaerobic and aerobic metabolism. Mean lactate levels decreased significantly during MP for all 3 groups (Fig. 2C). At 120 minutes of MP, mean perfusate lactate levels were lower for the MPRT group than the MP37 and MP30 groups, but by 240 minutes of MP, there were no significant differences between groups.

At the end of reperfusion, a trend toward lower mean lactate levels was observed for MPRT and SCS groups, although this did not reach statistical significance ($P = 0.05$, MPRT versus MP30; $P = 0.11$, MPRT versus MP37; $P = 0.08$, SCS versus MP30; Fig. 2D).

Bile Production and Biliary Glucose Reflect Graft Function During MP and Reperfusion

The quantity and characteristics of the bile produced by the graft are emerging as biomarkers of graft viability. Total bile production was measured as an indicator of graft metabolic function. Biliary glucose levels were measured as an indicator of biliary epithelial function, with lower glucose levels resulting from increased reabsorption by a functional biliary epithelium.^(17,18)

During 4 hours of MP, mean bile production correlated with metabolic rate, with the greatest quantity of bile produced by the MP37 group (Fig. 2E). Biliary glucose levels were also lowest for the MP37 group, indicating more normal activity of the biliary epithelium (Fig. 2F).

Interestingly, during graft reperfusion, opposite trends were observed. Mean bile production was most robust for livers that had been preserved by MPRT ($P = 0.006$, MPRT versus MP37; Fig. 2E). Biliary glucose levels also trended lower in this group, although this did not reach significance ($P = 0.06$, MPRT versus MP30; Fig. 2F).

INDICES OF GRAFT INJURY DURING MP AND REPERFUSION

Transaminase Release Remains Low During MP but Increases During Reperfusion According to Preservation Conditions

AST and ALT were measured during MP and reperfusion as indicators of hepatocellular injury. During MP, there was a time-dependent increase in both mean AST and mean ALT, although absolute levels remained low for all groups (Fig. 3A,B). During graft reperfusion, a more robust release of AST and ALT was observed. Mean AST and ALT were highest for livers preserved by MP37 with lower levels observed in the MP30, MPRT, and SCS groups (Fig. 3A,B).

Biliary LDH Levels Are Low During MP but Increase Significantly During Reperfusion in Livers Preserved by MP at 37°C

Biliary LDH was measured as an indicator of cell death of the biliary epithelium.⁽¹⁹⁾ Following MP, biliary LDH levels were low for all 3 groups (Fig. 3C). Following reperfusion, biliary LDH was significantly elevated in the MP37 group compared with the MPRT group ($P = 0.008$, MPRT versus MP37; Fig. 3C).

Vascular Resistance Remains Stable During MP but Increases During Reperfusion in Livers Preserved by MP at Both 30°C and 37°C

Vascular resistance in the graft was measured as a surrogate for microvascular injury.⁽²⁰⁾ During 4 hours of MP, mean vascular resistance remained stable for all 3 groups ($P =$ not significant, 10 versus 240 minutes). Between groups, there were no significant differences observed in mean vascular resistance at any time point during MP (Fig. 3D).

During graft reperfusion, a significant increase in mean vascular resistance was observed for both MP30 and MP37 groups in comparison to MPRT and SCS. This difference reached statistical significance by 90 minutes of reperfusion (Fig. 3E).

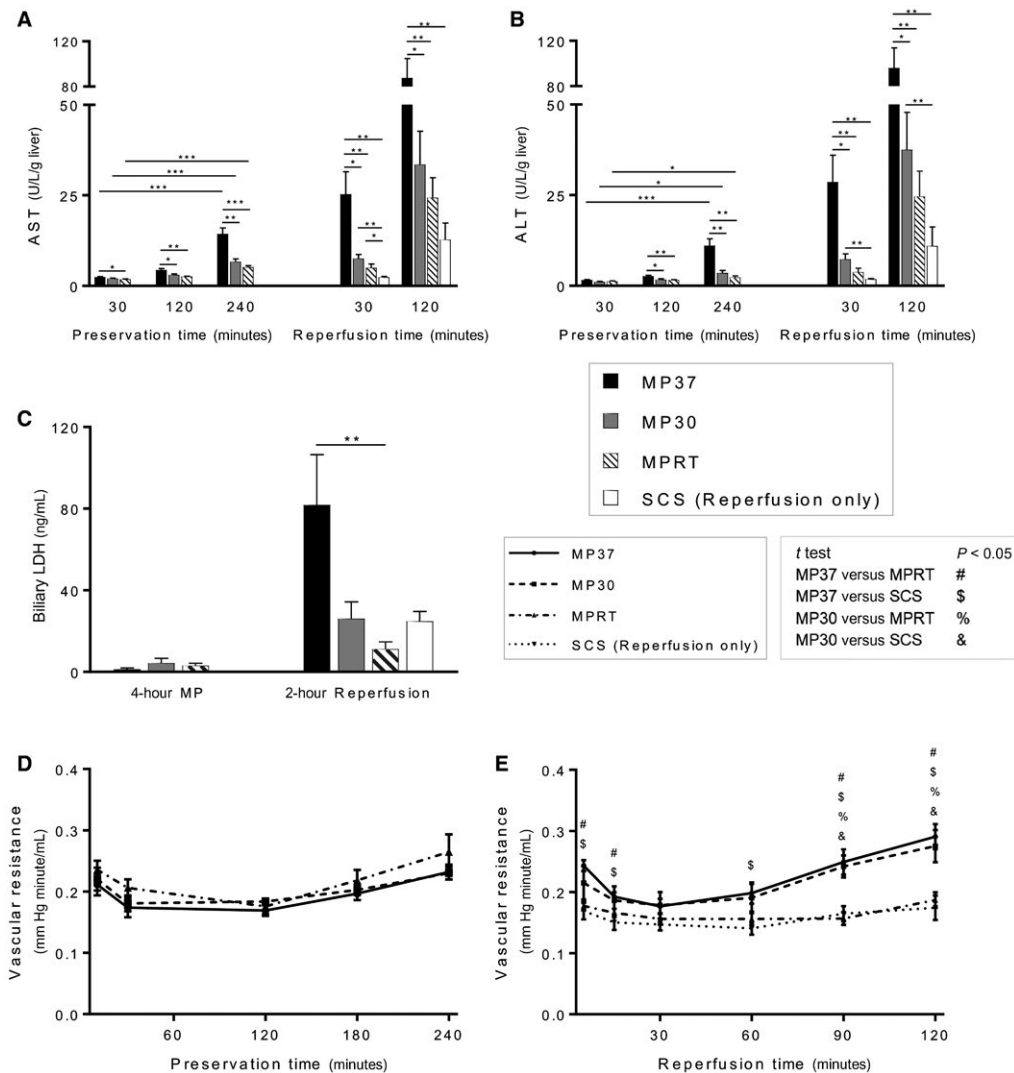


FIG. 3. Graft injury during MP and reperfusion. (A) AST and (B) ALT levels remained low during MP, although there was a time-dependent increase for all groups. Transaminase release during reperfusion was significantly higher in the MP37 group. (C) Biliary LDH levels were low during MP, but after reperfusion, they were significantly elevated in the MP37 group, indicative of biliary epithelial cell death. (D) Vascular resistance during MP was not significantly different between groups. (E) During reperfusion, vascular resistance was higher for the MP30 and MP37 groups, indicative of microvascular injury. Data are shown as mean \pm SEM, $n = 6$ per group. * $P < 0.05$, ** $P < 0.01$, *** $P < 0.001$.

INFLAMMATORY MOLECULES RELEASED DURING MP AND THEIR BIOLOGIC EFFECTS

Time-Dependent Increase in DAMP Levels During MP

HMGB1 and exDNA are 2 DAMPs that have been previously characterized in liver I-R injury and were thus selected for analysis.^(21,22) During MP, a

time-dependent increase in mean HMGB1 level was observed for all 3 groups (Fig. 4A). At 120 minutes of MP, levels of HMGB1 were significantly higher in the MP37 group ($P = 0.04$, MP37 versus MPRT). Similarly, a time-dependent increase in mean exDNA levels was observed for all groups (Fig. 4B). The rate of rise appeared to be more rapid for the MP37 and MP30 groups, and by 4 hours of MP, there was a significantly lower level of exDNA in the MPRT group (Fig. 4B).

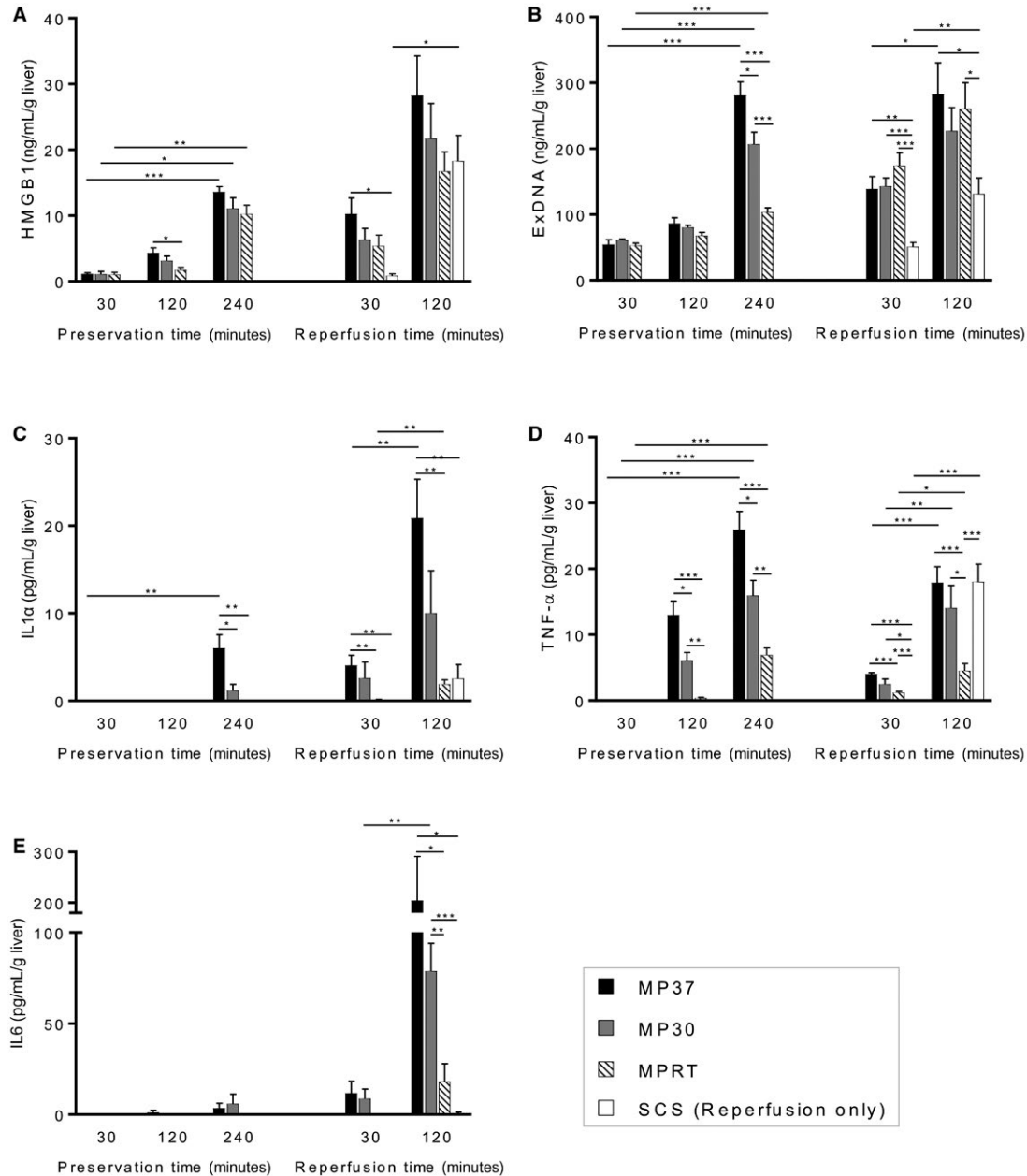


FIG. 4. Time-dependent increase in DAMPs and inflammatory cytokines during MP. (A) HMGB1 and (B) exDNA levels increased during MP for all groups with absolute levels correlating with temperature and graft metabolism. During MP, levels of (C) IL1 α and (D) TNF- α increased with time and correlated with temperature and graft metabolism. During reperfusion, (C) IL1 α and (E) IL6 were lowest for the MPRT and SCS groups, but (D) TNF- α was elevated in grafts that had been preserved by SCS. Data are shown as mean \pm SEM, n = 6 per group. * P < 0.05, ** P < 0.01, *** P < 0.001.

During graft reperfusion, a rapid increase in the mean HMGB1 level was observed for the SCS group, which was the only group to demonstrate a significant increase between 30 and 120 minutes ($P = 0.03$;

Fig. 4A). At the end of reperfusion, there were no differences in mean HMGB1 levels observed between groups. A significant increase in mean exDNA level was also observed for the SCS group ($P = 0.010$;

Fig. 4B) and MP37 group ($P = 0.02$; Fig. 4B). At the end of reperfusion, mean exDNA levels were lowest for the SCS group (Fig. 4B).

Time-Dependent Increase in Inflammatory Cytokines During MP

During MP, a time-dependent increase was observed for levels of IL1 α (for MP37) and TNF- α (for all groups). Cytokine levels correlated with graft metabolic rate with highest mean levels in the MP37 group and a stepwise reduction in levels for the MP30 and MPRT groups (Fig. 4C,D). IL6 levels remained low for all groups during MP (Fig. 4E).

During reperfusion, a time-dependent increase was observed for levels of IL1 α (MP37 and MPRT groups), TNF- α (all groups), and IL6 (MP30 group). Mean levels of IL1 α and IL6 were highest in the MP37 group (Fig. 4C,E). Interestingly, TNF- α exhibited a different pattern with mean levels increasing most rapidly in the SCS group. By the end of reperfusion, TNF- α levels were significantly higher for the MP37, MP30, and SCS groups in comparison to the MPRT group (Fig. 4D).

Biologically Active DAMPs Released During MP Stimulate TLRs

To assess the biological activity of DAMPs released into the perfusate, an in vitro assay was performed using commercially available TLR reporter cell lines. In this assay, TLR stimulation produces activation of NF- κ B, which is reflected by secretion of alkaline phosphatase in the cell media and detected by a colorimetric assay.⁽²³⁾ Perfusate samples were incubated with TLR3, TLR4, and TLR9 reporter cell lines, which are activated by extracellular RNA, HMGB1, and exDNA, respectively.^(24,25)

Perfusate samples from the end of MP demonstrated differential capacity for TLR stimulation with significantly increased activation of TLR3 and TLR9 by perfusate from the MP37 group (Fig. 5A,C). There was also a trend toward increased TLR4 stimulation by the MP37 group, but this did not reach statistical significance ($P = 0.07$, MP37 versus MPRT; $P = 0.12$, MP37 versus MP30; Fig. 5B). Similar trends were observed at the end of reperfusion with significantly higher TLR3 and TLR9 activation by the MP37 group compared with the MPRT and SCS groups (Fig. 5A,C).

Gene Expression Related to Inflammation, Oxidative Stress, TLR Signaling, and the Inflammasome Correlates With Levels of Inflammatory Molecules During MP

Following graft reperfusion, RNA was isolated from the tissue and gene expression analysis performed for a panel of inflammatory genes. Of particular interest were those related to priming of the NLRP3 inflammasome, which occurs in response to binding of IL1, TNF- α , and DAMPs to their respective receptors.⁽²⁶⁾

GENERAL INFLAMMATION

The induction of generalized inflammation was determined by measuring IL6 and TNF gene expression. A significant increase in expression of IL6 was observed in the MP37 group compared with the MPRT and SCS groups. No significant differences in gene expression were observed for TNF- α (Fig. 6A).

OXIDATIVE STRESS

The degree of oxidative stress was determined by expression of HO-1 and SOD-2, 2 cytoprotective enzymes responsive to cellular stress. HO-1 expression was significantly increased in the MP37 group in comparison to the other MP groups and SCS. No differences in gene expression were observed for SOD-2 (Fig. 6B).

TLR SIGNALING

The activity of TLR signaling pathways was determined by expression of MyD88, a cytosolic adaptor protein that acts as a key intermediary in the TLR signaling cascade, and NF- κ B, a downstream product of TLR activation. MyD88 gene expression was significantly increased in the MP37 group compared with the MP30 and SCS groups. Similarly, increased expression of NF- κ B was observed in the MP37 group compared with the MPRT and SCS groups (Fig. 6C).

NLRP3 INFLAMMASOME

Priming of the NLRP3 inflammasome was compared by determining expression of NLRP3 and

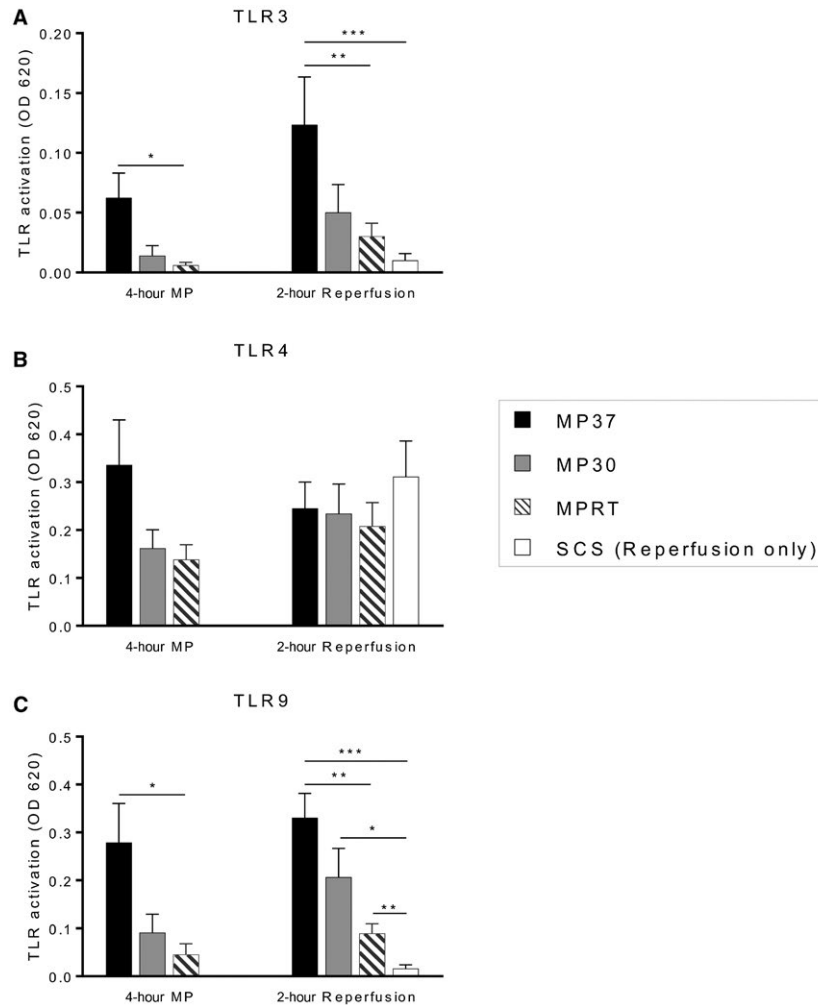


FIG. 5. DAMPs released during MP and graft reperfusion are biologically active and stimulate TLRs. Perfusate samples at the end of MP and end of reperfusion were incubated with TLR reporter cell lines. TLR stimulation produces activation of NF- κ B, which is linked to secretion of alkaline phosphatase into the cell media and detected by a colorimetric assay. (A) TLR3 activation, indicative of binding by double-stranded RNA. (B) TLR4 activation, indicative of binding by HMGB1. (C) TLR9 activation, indicative of binding by exDNA. Data are shown as mean \pm SEM, $n = 6$ per group. * $P < 0.05$, ** $P < 0.01$, *** $P < 0.001$.

pro-IL1 β . Both of these key components of the inflammasome are up-regulated in response to binding of IL1, TNF- α , and DAMPs to their respective receptors.^(26,27)

A significant reduction in NLRP3 expression was observed in the MPRT group compared with MP37, indicating reduced inflammasome priming ($P = 0.04$; Fig. 6D). There was also a trend toward decreased NLRP3 expression in the MPRT group compared with SCS ($P = 0.11$). Similarly, pro-IL1 β gene expression was significantly lower in the MPRT group compared with MP37 ($P = 0.048$; Fig. 6D).

Increased Histologic Injury and Apoptosis Following Reperfusion Correlates With Levels of Inflammatory Molecules During MP

Histology was performed at the end of graft reperfusion, including standard H & E and immunohistochemistry for cleaved caspase 3 and TUNEL. Qualitatively, liver architecture appeared most normal in the MPRT group (Fig. 7B). The MP30 and MP37 groups demonstrated increased hepatocyte

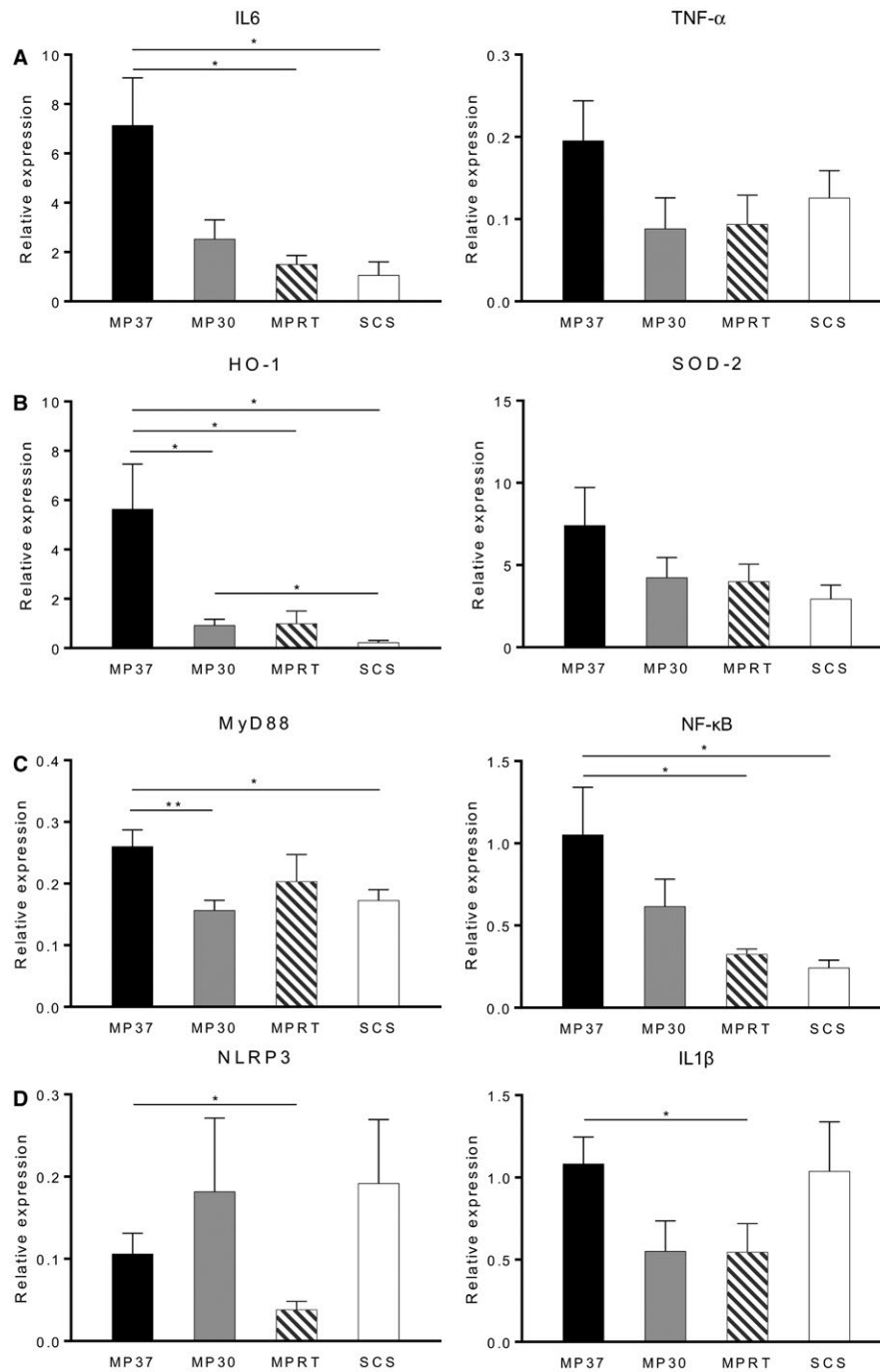


FIG. 6. Gene expression related to (A) generalized inflammation, (B) oxidative stress, (C) TLR signaling, and (D) inflammasome priming. Gene expression analysis was performed on graft tissue following 4 hours of preservation and 2 hours of reperfusion. IL6, HO-1, MyD88, and NF- κ B were up-regulated in the MP37 group. Inflammasome genes NLRP3 and pro-IL1 β were down-regulated in the MPRT group. Data are shown as mean \pm SEM, $n = 6$ per group. * $P < 0.05$, ** $P < 0.01$.

vacuolization, congestion, and necrosis, reflected by a significant increase in the Suzuki score for assessment of liver damage (Fig. 7C).

There were lower levels of cleaved caspase 3 staining present in the MPRT and SCS groups in comparison to the MP37 and MP30 groups. The degree

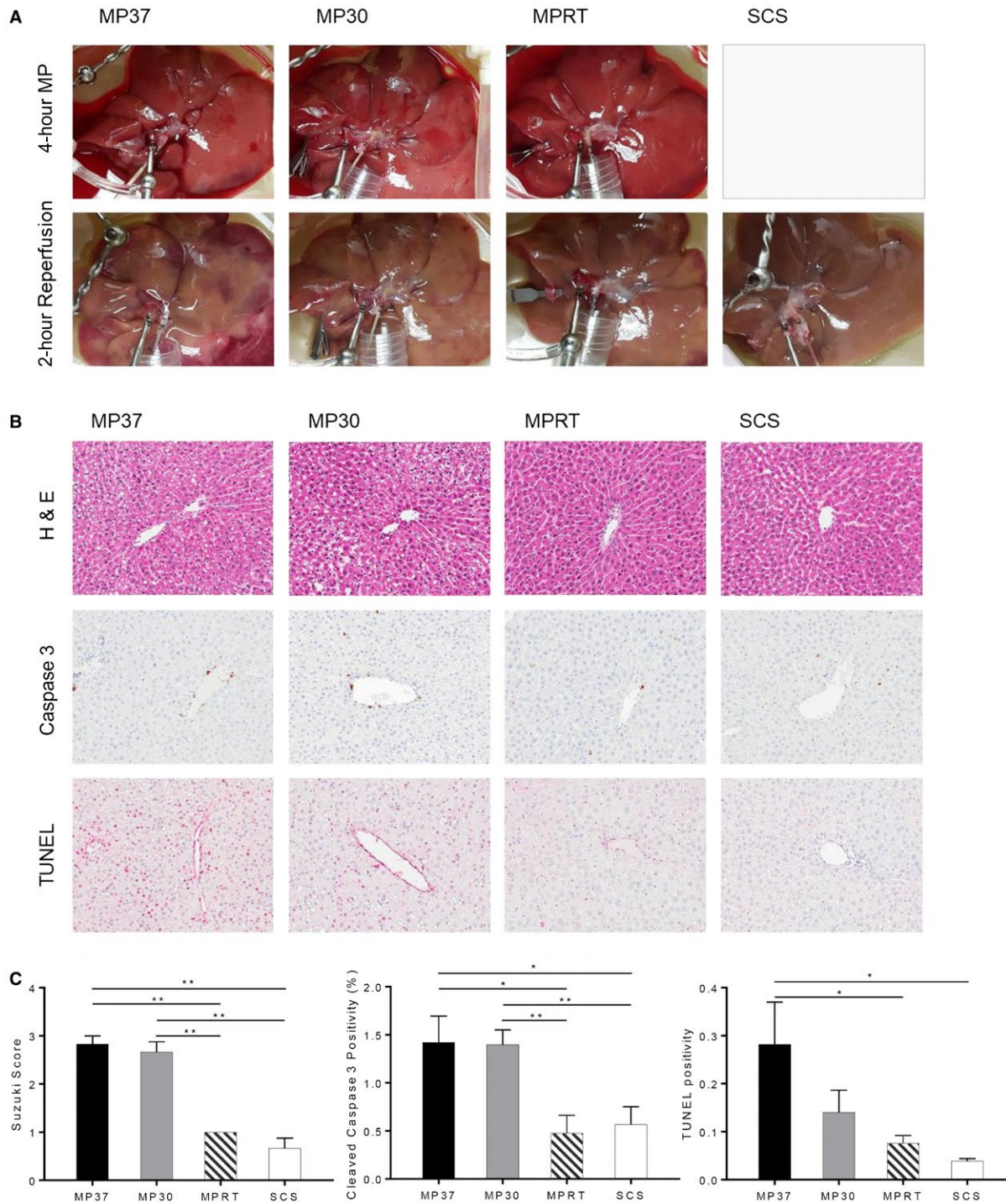


FIG. 7. Histologic injury and apoptosis following reperfusion. Histology was performed at the end of graft reperfusion, including standard H & E and immunohistochemistry for cleaved caspase 3 and TUNEL. (A) Gross appearance of grafts during MP and reperfusion. (B) H & E and immunohistochemistry staining. (C) Quantitative analysis of graft injury and apoptosis by Suzuki score, cleaved caspase 3, and TUNEL staining. Data are shown as mean \pm SEM, $n = 6$ per group for H & E, $n = 5$ per group for immunohistochemistry. * $P < 0.05$, ** $P < 0.01$.

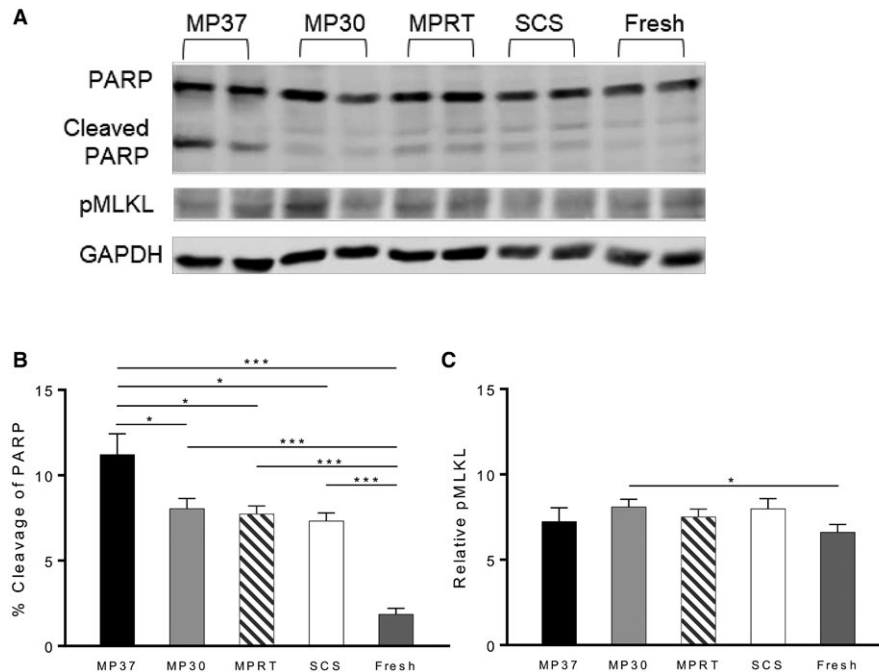


FIG. 8. Apoptosis, not necroptosis, is the dominant type of programmed cell death following graft reperfusion. (A) Western blot analysis performed on tissue lysates following graft reperfusion. Lysates were probed with anti-PARP or anti-MLKL antibodies, indicative of apoptosis and necroptosis, respectively. (B) Apoptosis is significantly increased in all experimental groups over fresh liver tissue. Among experimental groups, apoptosis is highest in the MP37 group. (C) Necroptosis is minimally increased in experimental groups over fresh tissue. Data are shown as mean \pm SEM, $n = 6$ per group. * $P < 0.05$, *** $P < 0.001$.

of TUNEL staining was also significantly lower in the MPRT and SCS groups in comparison to the MP37 group (Fig. 7C).

Apoptosis, Not Necroptosis, Is the Dominant Type of Programmed Cell Death Following Reperfusion

Both apoptosis and necroptosis are stimulated by TNF- α binding to TNF receptor 1,⁽²⁸⁾ although the relative activity of these regulated cell death pathways during reperfusion remains unknown. To test this, protein lysates were prepared following graft reperfusion and probed for cleaved PARP and phosphorylated mixed lineage kinase domain-like protein (pMLKL), specific markers for apoptosis and necroptosis, respectively.

A greater degree of apoptosis was evident in the MP37 group compared with the other MP groups and SCS. All experimental groups displayed significantly more apoptosis than the fresh tissue control, as expected (Fig. 8B). In contrast, a similar degree of necroptosis was present in all experimental groups, which was not

significantly greater than the fresh tissue control, with the exception of the MP30 group (Fig. 8C).

Discussion

Although MP has emerged as a promising technology in liver transplantation, the cellular processes occurring in this environment remain undefined. In this study, we demonstrate a time-dependent increase in levels of DAMPs and inflammatory cytokines during MP, more pronounced at higher preservation temperatures and increased graft metabolism (Fig. 4). Moreover, we demonstrate that elevated levels of these inflammatory molecules during MP are associated with increased activation of TLRs (Fig. 5), priming of the NLRP3 inflammasome (Fig. 6), and apoptosis following graft reperfusion (Figs. 7 and 8).

From a mechanistic perspective, the findings in our study suggest that DAMPs act as key mediators of inflammation during MP. We demonstrate the ability of these DAMPs to stimulate TLRs, which are present on a variety of cell types in the liver including Kupffer

cells, dendritic cells, hepatocytes, biliary epithelial cells, and sinusoidal endothelial cells.⁽²⁹⁾ TLR activation leads to the production of inflammatory cytokines including IL1 α and TNF- α , as demonstrated in our study. Signaling via TLRs, the IL1 receptor, and TNF receptor 1 leads to priming of the NLRP3 inflammasome through increased gene expression of NLRP3 and pro-IL1 β .⁽²⁶⁾ We observed evidence of differential inflammasome priming in our study with significantly lower levels of priming in grafts preserved by MP at room temperature. In parallel, increased levels of TNF lead to the induction of apoptosis via binding to TNF receptor 1,⁽³⁰⁾ and we observed a strong correlation between circulating TNF levels during MP and apoptosis following graft reperfusion.

Although our primary focus was on defining the biological activity of DAMPs and cytokines released during MP, we also demonstrated that reducing graft metabolism by lowering the preservation temperature mitigated MP-associated inflammation. This finding is consistent with a recent study by Goldaracena et al., which demonstrated lower levels of IL6 and TNF- α during MP at 33°C compared with 37°C in a porcine model.⁽⁷⁾ At present, there is ongoing debate about the “optimal” temperature for MP (hypothermic, subnormothermic, or normothermic), which is beyond the scope of this study. Each temperature has particular advantages and disadvantages, and in the future, we envision the use of temperature as a fluid parameter to manipulate graft metabolism for specific purposes. An example of such a scenario is the initial use of a normothermic environment to promote uptake and activity of a therapeutic agent, followed by a period of extended preservation at a lower temperature to reduce metabolism and inflammation.

The time-dependent increase in inflammatory molecules observed in this study demonstrates a current limitation of MP systems. In vivo, DAMPs and cytokines have short circulating half-lives due to the activity of plasma enzymes and renal filtration.⁽³¹⁻³³⁾ In contrast, MP devices lack these mechanisms of clearance, which may result in prolonged circulation and activity of inflammatory molecules during MP. Our findings demonstrate that DAMPs released during MP have a deleterious impact on the graft by inciting a feed-forward cycle of inflammation and further cell injury. This is consistent with a recent study by Hashimoto et al., who demonstrated an association between elevated levels of circulating DAMPs during MP and primary graft dysfunction following human

lung transplantation.⁽⁹⁾ We believe strategies to attenuate this inflammatory cycle have significant potential to improve outcomes with MP technology. Examples of such interventions include removal of circulating DAMPs and cytokines, inhibition of TLR signaling, and specific inhibitors of the inflammasome.^(34,35)

There are several limitations of this study that should be recognized. First, this is a rat model system and our findings require confirmation in larger animal models and humans. Second, we preserved healthy donor livers for a relatively short period of time (4 hours). Under these conditions, SCS remains a very effective mode of preservation and causes little graft injury. As such, we did not expect to demonstrate a significant advantage of MP over SCS with our study design. The deleterious effects of SCS are likely to be more evident in extended criteria grafts subjected to more prolonged cold storage preservation, as seen in the recent clinical trial by Nasralla et al.⁽⁶⁾ Despite the conditions in our study favoring SCS, after reperfusion, we observed substantial TNF- α release and a trend toward increased inflammasome priming in SCS grafts ($P = 0.11$ for NLRP3 expression, SCS versus MPRT). These mechanisms of cold storage injury require further investigation. Third, graft reperfusion was achieved by ex vivo reperfusion with an acellular perfusate (Krebs-Henseleit solution). We selected this model because it is the standard model for ex vivo reperfusion experiments in the literature.^(20,36-40) However, we certainly acknowledge that rat liver transplantation is the optimal reperfusion model and are refining our technique for future studies. Finally, we used a model with isolated portal inflow. Although this is a well-established model described in numerous studies, it is unknown how the lack of arterial inflow may impact our findings.

In conclusion, MP in liver transplantation has entered the clinical arena with promising results in a recent European randomized clinical trial.⁽⁶⁾ Thus far, clinical progress has outpaced our understanding of the biological processes occurring in the MP environment. Our findings in this study indicate that DAMP-mediated inflammation during MP negatively impacts the graft. Subsequent studies are required to determine how these processes affect extended criteria grafts from elderly, steatotic, and donation after circulatory death donors. Taken together, our findings suggest that strategies to address DAMP-mediated inflammation during MP can further optimize this promising technology.

Acknowledgments: We thank the members of the Duke Transplant Laboratory for their assistance in critical discussion and refinement of this study.

REFERENCES

- Guarrera JV, Henry SD, Samstein B, Odeh-Ramadan R, Kinkhabwala M, Goldstein MJ, et al. Hypothermic machine preservation in human liver transplantation: the first clinical series. *Am J Transplant* 2010;10:372-381.
- Guarrera JV, Henry SD, Samstein B, Reznik E, Musat C, Lukose TI, et al. Hypothermic machine preservation facilitates successful transplantation of "orphan" extended criteria donor livers. *Am J Transplant* 2015;15:161-169.
- Dutkowski P, Schlegel A, de Oliveira M, Müllhaupt B, Neff F, Clavien PA. HOPE for human liver grafts obtained from donors after cardiac death. *J Hepatol* 2014;60:765-772.
- Ravikumar R, Jassem W, Mergental H, Heaton N, Mirza D, Perera MT, et al. Liver transplantation after ex vivo normothermic machine preservation: a phase 1 (first-in-man) clinical trial. *Am J Transplant* 2016;16:1779-1787.
- Selzner M, Goldaracena N, Echeverri J, Kathis JM, Linares I, Selzner N, et al. Normothermic ex vivo liver perfusion using steen solution as perfusate for human liver transplantation: first North American results. *Liver Transpl* 2016;22:1501-1508.
- Nasralla D, Coussios CC, Mergental H, Akhtar MZ, Butler AJ, Ceresa CDL, et al.; for Consortium for Organ Preservation in Europe. A randomized trial of normothermic preservation in liver transplantation. *Nature* 2018;557:50-56.
- Goldaracena N, Echeverri J, Spetzler VN, Kathis JM, Barbas AS, Louis KS, et al. Anti-inflammatory signaling during ex vivo liver perfusion improves the preservation of pig liver grafts before transplantation. *Liver Transpl* 2016;22:1573-1583.
- Noda K, Tane S, Haam SJ, D'Cunha J, Hayanga AJ, Luketich JD, Shigemura N. Targeting circulating leukocytes and pyroptosis during ex vivo lung perfusion improves lung preservation. *Transplantation* 2017;101:2841-2849.
- Hashimoto K, Cypel M, Juvet S, Saito T, Zamel R, Machuca TN, et al. Higher M30 and high mobility group box 1 protein levels in ex vivo lung perfusate are associated with primary graft dysfunction after human lung transplantation. *J Heart Lung Transplant* 2017; <https://doi.org/10.1016/j.healun.2017.06.005>.
- Braza F, Brouard S, Chadban S, Goldstein DR. Role of TLRs and DAMPs in allograft inflammation and transplant outcomes. *Nat Rev Nephrol* 2016;12:281-290.
- Land WG, Agostinis P, Gasser S, Garg AD, Linkermann A. Transplantation and damage-associated molecular patterns (DAMPs). *Am J Transplant* 2016;16:3338-3361.
- Tolboom H, Pouw R, Uygun K, Tanimura Y, Izamis ML, Berthiaume F, Yarmush ML. A model for normothermic preservation of the rat liver. *Tissue Eng* 2007;13:2143-2151.
- Op den Dries S, Karimian N, Westerkamp AC, Sutton ME, Kuipers M, Wiersma-Buist J, et al. Normothermic machine perfusion reduces bile duct injury and improves biliary epithelial function in rat donor livers. *Liver Transpl* 2016;22:994-1005.
- Suzuki S, Toledo-Pereyra LH, Rodriguez FJ, Cejalvo D. Neutrophil infiltration as an important factor in liver ischemia and reperfusion injury. Modulating effects of FK506 and cyclosporine. *Transplantation* 1993;55:1265-1272.
- Sun X, Zhang Y, Wang J, Wei L, Li H, Hanley G, et al. Beta-arrestin 2 modulates resveratrol-induced apoptosis and regulation of Akt/GSK3 β pathways. *Biochim Biophys Acta* 2010;1800:912-918.
- McLellan SA, Walsh TS. Oxygen delivery and haemoglobin. *Continuing Education Anaesthesia Crit Care Pain* 2004;4:123-126.
- Lira M, Schteingart CD, Steinbach JH, Lambert K, McRoberts JA, Hofmann AF. Sugar absorption by the biliary ductular epithelium of the rat: evidence for two transport systems. *Gastroenterology* 1992;102:563-571.
- Wu CT, Davis PA, Luketic VA, Gershwin ME. A review of the physiological and immunological functions of biliary epithelial cells: targets for primary biliary cirrhosis, primary sclerosing cholangitis and drug-induced ductopenias. *Clin Dev Immunol* 2004;11:205-213.
- Vajdová K, Smreková R, Kukan M, Lutterová M, Wsólóvá L. Bile analysis as a tool for assessing integrity of biliary epithelial cells after cold ischemia-reperfusion of rat livers. *Cryobiology* 2000;41:145-152.
- Besems M, 't Hart NA, Tolba R, Doorschodt BM, Leuvenink HG, Ploeg R, et al. The isolated perfused rat liver: standardization of a time-honoured model. *Lab Anim* 2006;40:236-246.
- Bamboot ZM, Balachandran VP, Ocuin LM, Obaid H, Plitas G, DeMatteo RP. Toll-like receptor 9 inhibition confers protection from liver ischemia-reperfusion injury. *Hepatology* 2010;51:621-632.
- Brenner C, Galluzzi L, Kepp O, Kroemer G. Decoding cell death signals in liver inflammation. *J Hepatol* 2013;59:583-594.
- Lee J, Jackman JG, Kwun J, Manook M, Moreno A, Elster EA, et al. Nucleic acid scavenging microfiber mesh inhibits trauma-induced inflammation and thrombosis. *Biomaterials* 2017;120:94-102.
- Yu L, Wang L, Chen S. Endogenous toll-like receptor ligands and their biological significance. *J Cell Mol Med* 2010;14:2592-2603.
- Kiziltas S. Toll-like receptors in pathophysiology of liver diseases. *World J Hepatol* 2016;8:1354-1369.
- He Y, Hara H, Núñez G. Mechanism and regulation of NLRP3 inflammasome activation. *Trends Biochem Sci* 2016;41:1012-1021.
- Latz E, Xiao TS, Stutz A. Activation and regulation of the inflammasomes. *Nat Rev Immunol* 2013;13:397-411.
- Zhao H, Jaffer T, Eguchi S, Wang Z, Linkermann A, Ma D. Role of necroptosis in the pathogenesis of solid organ injury. *Cell Death Dis* 2015;6:e1975.
- Mencin A, Kluwe J, Schwabe RF. Toll-like receptors as targets in chronic liver diseases. *Gut* 2009;58:704-720.
- Parameswaran N, Patial S. Tumor necrosis factor- α signaling in macrophages. *Crit Rev Eukaryot Gene Expr* 2010;20:87-103.
- Andres-Hernando A, Dursun B, Altmann C, Ahuja N, He Z, Bhargava R, et al. Cytokine production increases and cytokine clearance decreases in mice with bilateral nephrectomy. *Nephrol Dial Transplant* 2012;27:4339-4347.
- Betjes MG. Immune cell dysfunction and inflammation in end-stage renal disease. *Nat Rev Nephrol* 2013;9:255-265.
- Tecklenborg J, Clayton D, Siebert S, Coley SM. The role of the immune system in kidney disease. *Clin Exp Immunol* 2018;192:142-150.
- Guo H, Callaway JB, Ting JP. Inflammasomes: mechanism of action, role in disease, and therapeutics. *Nat Med* 2015;21:677-687.
- Lamkanfi M, Mueller JL, Vitari AC, Misaghi S, Fedorova A, Deshayes K, et al. Glyburide inhibits the Cryopyrin/Nalp3 inflammasome. *J Cell Biol* 2009;187:61-70.
- Berardo C, Di Pasqua LG, Siciliano V, Rizzo V, Richelmi P, Ferrigno A, Vairetti M. Machine perfusion at 20°C prevents

ischemic injury and reduces hypoxia-inducible factor-1 α expression during rat liver preservation. *Ann Transplant* 2017;22:581-589.

- 37) Okamura Y, Hata K, Tanaka H, Hirao H, Kubota T, Inamoto O, et al. Impact of subnormothermic machine perfusion preservation in severely steatotic rat livers: a detailed assessment in an isolated setting. *Am J Transplant* 2017;17:1204-1215.
- 38) Vairetti M, Ferrigno A, Carlucci F, Tabucchi A, Rizzo V, Boncompagni E, et al. Subnormothermic machine perfusion

protects steatotic livers against preservation injury: a potential for donor pool increase? *Liver Transpl* 2009;15:20-29.

- 39) Vairetti M, Ferrigno A, Rizzo V, Richelmi P, Boncompagni E, Neri D, et al. Subnormothermic machine perfusion protects against rat liver preservation injury: a comparative evaluation with conventional cold storage. *Transplant Proc* 2007;39:1765-1767.
- 40) Ferrigno A, Carlucci F, Tabucchi A, Tommassini V, Rizzo V, Richelmi P, et al. Different susceptibility of liver grafts from lean and obese Zucker rats to preservation injury. *Cryobiology* 2009;59:327-334.